Desalination and Water Treatment
www.deswater.com
29 (2011) 149–157
May
1944-3994 / 1944-3986 © 2011 Desalination Publications. All rights reserved.
doi: 10.5004/dwt.2011.1373

Preventing formation of dry patches in seawater falling film evaporators

J. Mitrovic*

Institute of Technical Thermodynamics and Thermal Process Engineering, University of Stuttgart, 70550 Stuttgart, Germany
Tel. +49 7157 705569; email: mitrovic@tebam.de

Received 28 April 2009; Accepted in revised form 28 November 2010

ABSTRACT

When a liquid film is falling across a heated surface, the film structure results in a variation of heat transfer and interface temperature thus facilitating the film rupture. The variation of heat transfer lefts behind a thermal topology on the heating surface that may suffice to initiate formation of vapour bubbles. Once formed, vapour bubbles grow and act on the film flow as obstacles, disturb the film and may cause film rupture with stable dry patches and salt deposition on the heating surface. Even if the liquid film remains continuous, any growing bubble results in salt deposition on the heating surface in the bubble foot region, and in both cases the heat transfer in the film becomes deteriorated. Consequently, bubble formation in evaporating falling films is to be prevented in the praxis. In the present contribution first the conditions of bubble nucleation in an evaporating falling film are formulated. From these conditions the minimum heating surface temperature required for nucleate boiling in the film is determined. This temperature is considered to represent the upper limit for the convective heat transfer in the film without bubble formation. The obtained results are illustrated in the second part of the paper, adopting a falling film evaporator equipped with horizontal tubes as example. The tubes, arranged one below the other and sprayed outside with seawater, are heated inside by condensing vapour.

Keywords: Falling film; Bubble nucleation; Dry patches; Heat transfer

1. Introduction

Falling film evaporators are frequently encountered in processes of thermal engineering like food industry, pharmaceutical industry and seawater desalination. In these processes, the falling film is separated from the heating fluid by a wall that may be designed e.g. as a plane or wavy plate, and a plain tube having an elliptical or circular cross-section. In seawater desalination processes, the heating fluid is usually condensing steam generated in the previous effect and enhanced in a thermal compression process. The seawater enters the evaporator as saturated or subcooled liquid. In the later case, the water is heated first without a vapour generation on the film surface. With saturated liquid, the situation is insofar different as evaporation starts sooner with respect to the distance to film inlet. In both cases, however, the evaporation on the film surface requires the thermal boundary layer, developing in the film, to reach the film surface. Upstream this position, the film portion is thermally non-developed, while downstream, it is usually considered as thermally developed.

In the thermally developed film region, the mass flux leaving the film surface, is given by

* Actual office address: University of East Sarajevo, Faculty for Production and Management Trebinje, Stepe Stepanovica bb, 89191 Trebinje, Republic of Srpska, Bosnia and Herzegovina.

$$\dot{m} = \frac{q}{\Delta h} = \frac{k}{\Delta h}\left(T_{\mathrm{COND}} - T_{\mathrm{EVAP}}\right) \quad (1)$$

where q is the wall heat flux, k is the overall heat transfer coefficient, Δh is the latent heat of evaporation, and $T_{\mathrm{COND}} - T_{\mathrm{EVAP}}$ is the overall driving temperature difference.

The quantity k takes into account the thermal resistances of condensate, falling film and of the separating wall:

$$\frac{1}{k} = \frac{1}{\alpha_{\mathrm{COND}}} + \frac{\delta_W}{\lambda_W} + \frac{1}{\alpha_{\mathrm{EVAP}}} \quad (2)$$

As follows from Eqs. (1) and (2), the evaporation rate depends on the kinetics of heat transfer and on the thermal potentials of the separating wall and the fluids thermally communicating with each other. The convection thermal resistances, the inverses of the heat transfer coefficients α_{COND} and α_{EVAP}, are complex functions of flow states of the phases, their physical properties, and the shape of the heating surface.

As Eqs. (1) and (2) tell, two largely independent ways are possible to increase the evaporation rate:

- increase in the overall heat transfer coefficient k, and/or
- increase in the driving temperature difference.

The possibilities and achievements along these ways are limited. The limitations are associated with the evaporation of the film and arise from the process economy, on one side, and from the film rupture, on the other. High heat transfer coefficients of evaporating films establish at a small film thickness. Such films, however, are inclined to breakdown and dry patches thus formed reduce the size of the wetted surface area and reinforce scale formation. High heat transfer coefficients are also possible at a larger film flow rate. However, large water flow rates require stronger thermal engagement; the energy excess leaving the process with the brine as waste heat increases, substantially affecting both the environment and the thermal economy of the process.

Increasing the driving temperature difference raises the evaporation rate, provided that the overall heat transfer coefficient remains unchanged or at least decreases less than the increase of the temperature difference. In general, however, higher driving temperature difference facilitates the film rupture by interfacial (Marangoni) stresses which may indirectly limit the evaporation rate. In addition, a sufficiently large driving temperature difference causes formation of vapour bubbles on the heating surface. Once formed, vapour bubbles act as obstacles on the film flow and may cause the film rupture. Under reliable operation of falling film evaporators, formation of vapour bubbles is to be suppressed. However, at present, very little is known about the bubble formation in complex flows like falling films in seawater evaporators. Formation and growth of vapour bubbles in a film depends on a number of parameters like the physico-chemical state of the heating surface, the heat transfer in the film, and the surface temperature. The mutual interaction between the heat transfer and bubble nucleation results in a minimum wall temperature required by bubble equilibrium. This minimum wall temperature represents at the same time the maximum allowable wall temperature for the film evaporation without bubble formation.

The aim of the present paper is twofold: first, to shed some more light on the formation of vapour bubbles in a falling film and, second, to derive an expression for the maximum wall temperature prior to bubble formation thus specifying the heat transfer conditions without the film rupture arising from bubble inception. As example, a falling film evaporator consisting of horizontal tubes is considered. Steam condensing inside the tubes provides the required heat. For this configuration, an expression is derived for the maximum overall driving temperature difference without bubble formation and the results are illustrated for the selected process parameters.

2. Nucleation of vapour bubbles

Nucleate boiling of liquids has been the subject matter of a great number of studies. These studies cover questions ranging from the formation of stable bubble nuclei in metastable liquids, via bubble growth and departure to the heat transfer under various conditions. A state of the art can be obtained from review articles and monographs e.g. by Westwater [1], Nesis [2], Carey [3] and Collier and Thome [4], to name only a few. Hsu and Graham [5] were the first to provide a model for bubble generation in a liquid under heat transfer conditions. A paper by Mitrovic [6] gives a brief overview about the historical development of the ideas pertaining to bubble nucleation. From this paper, we may draw the following conclusions:

1. Inert gases, dissolved in the liquid, or adsorbed on the surface of the wall, affect bubble generation.
2. The boiling temperature (liquid superheat) depends on the amount of the dissolved gases, the surface roughness, and the interaction liquid-solid wall.
3. The bubble formation in a superheated liquid proceeds along different ways. At a strong superheat, the boiling manifests itself explosively.

These conclusions are basing on experimental observations. Theoretical contributions of fundamental importance in this area have been provided, among others, by William Thomson (Lord Kelvin) [7], J.W. Gibbs [8], and J.J. Thomson [9]. Adopting a thought experiment, Thomson [7] described the effect of curvature of the interface on vapour pressure, while Gibbs [8] introduced an energy barrier of bubble formation. Another Thomson, Joseph John, [9] derived an equation for the liquid superheat arising from the interface curvature [10].

The modern ideas in the field of bubble formation and boiling heat transfer mostly deal with specific phenomena such as fluctuation of the state parameters preceding bubble nucleation, an issue, which can be traced back to the time of van der Waals [11], and even of Boskovic [12]. The heat transfer to a growing bubble, adhering to a heater surface, occurs mainly in the region where all the phases involved (liquid, vapour, and solid) are interacting with each other and the heat flux may change its direction [13].

2.1. The origin of vapour bubble nuclei

Jakob and Fritz [14] seem to be the first to systematically investigate the wall effect on nucleate boiling heat transfer. Corty and Foust [15] reported heat transfer data obtained with different liquids boiling on surfaces of various polish, noting the micro roughness of the boiling surface to be one of the fundamental factors governing the heat transfer:

> *"It may be postulated that there exist cavities in the metallic surface and that in these cavities vapour is trapped after an earlier bubble has broken loosely. The trapped vapour then acts as the nucleus for the next bubble from the same spot.*
>
> *A vapour–filled cavity may act as nucleus for bubble formation as long as the superheat in the surface is high enough to support the vapour phase inside the cavity against the constrictive effect of surface tension in the phase boundary."*

These findings by Corty and Foust in 1955 (PhD dissertation of C. Corty 1951) concerning the vapour rest acting as the nucleus for the next bubble are in agreement with the ideas already developed by Aitken [16] in 1878. Corty and Foust applied an expression for the equilibrium temperature of a concave interface to a bubble in a cavity. This seems to be for the first time to specify the minimum wall superheat required by thermodynamics for a stable vapour bubble. Later on, Hsu and Graham [5,17] first, and afterwards many others, extended this idea to non–isothermal systems. We will use the Hsu relationship in a slightly modified form further below to derive an expression for the maximum allowable driving temperature difference in seawater falling film evaporators.

2.2. Bubble equilibrium and the wall temperature

To prevent confusion, it should be stated at the outset that the considerations to follow are resting on the assumption of a single component system. The presence of salt in seawater certainly affects the phase equilibrium the description of which necessitates deeper insights into thermodynamics of two-phase ionic systems, which but would blast the frame of the present paper. A possible line of treatment in case of an ideal system could be taken e.g. from Mitrovic [18]. In general, however, one may conclude that — depending on salt concentration — the common boiling point elevation will result in a larger driving teperature difference in comparison to pure water.

Adopting for the present considerations the hypothesis that a bubble is generated from the vapour rest remaining in a surface cavity after detachment of the preceding bubble, the equilibrium conditions of this vapour rest would then formulate a criterion for bubble nucleation. Griffith and Wallis [19] proposed such a criterion by the expression

$$r_{CR} = 2\frac{\sigma T_\infty}{\Delta h \rho_V \left(T_W - T_\infty\right)} \tag{3}$$

where r_{CR} denotes the radius of the cavity mouth, σ the surface tension, Δh the evaporation enthalpy, T the temperature, and ρ the density. The indices V, W and ∞ refer to liquid, to vapour and to a large distance from the wall, respectively.

The temperature difference $T_W - T_\infty$ in Eq. (3) represents the minimum wall superheat required by the thermodynamic equilibrium conditions for a concave curvature of the interface. Derived by J.J. Thomson in 1886 for the first time, it would be safe to term this equation Thomson's (J.J.) nucleation criterion.

As noted above, Hsu and Graham [5,17] were the first to investigate the bubble existence conditions in a system with temperature gradient. Their analysis starts from the (J.J. Thomson) equation for a bubble in a liquid of homogeneous temperature

$$T_B = T_\infty + 2\frac{\sigma T_\infty}{\Delta h \rho_V r_B} \tag{4}$$

where the index B refers to the bubble; this expression is identical to Eq. (3).

The fate of a bubble in a liquid of an inhomogeneous temperature will depend on its size and the place with regard to the temperature distribution. As illustrated in Fig. 1 for a liquid of a linear temperature distribution, all bubbles of the temperature T_B in the region between the wall and temperature T_L of the liquid were thermodynamically stable. By contrast, a bubble above the line

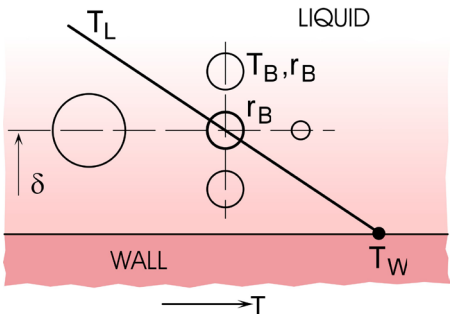

Fig. 1. Illustration of bubble survival conditions.

T_L is instable, and it would condense [20]. If the line T_L intersects the bubble interface, an evaporation–condensation process would occur, and the conditions of bubble growth would require

$$\frac{dm_V}{dt} = -\int_A \rho_L (u_{LI} - u_I) dA_B \geq 0 \tag{5}$$

where m_V is the mass of vapour forming the bubble, u_{LI} the radial velocity of the liquid at the interface moving at the velocity u_I, and A_B the interfacial surface area. This equation demands the evaporation to balance or to overcome the condensation, the liquid temperature T_L at the distance $\delta + r_B$ must thus at least be equal to the bubble temperature, T_B.

If the bubble is semi spherical and if it is attached to the mouth of a cavity of the radius, $r_C = r_B$, the temperature T_B in Eq. (4) can be plotted as a function of the wall distance $y = r_B$ (Fig. 2), see also [6,20].

For a linear temperature distribution in the liquid near the wall, it is

$$\frac{dT_L}{dy} = -\frac{q}{\lambda_L} \tag{6}$$

and the requirement of tangency gives

$$\frac{dT_L}{dy} = \frac{T_B - T_{WCR}}{r_{CR}} = -\frac{q}{\lambda_L} = -\frac{\alpha(T_{WCR} - T_\infty)}{\lambda_L} \tag{7}$$

or

$$T_{WCR} - T_\infty = 2\frac{\sigma T_\infty}{\Delta h \rho_V r_{CR}} \Big/ \left(1 - \frac{\alpha r_{CR}}{\lambda_L}\right) \tag{8}$$

were λ_L denotes the liquid thermal conductivity, α the heat transfer coefficient, and the index CR refers to the critical bubble (cavity) radius. The structure of this equation is identical to the one reported by Howell and Siegel [21].

Since $T_{WCR} - T_\infty > 0$, the denominator in Eq.(8) requires

$$\alpha < \alpha_{max} = \frac{\lambda_L}{r_{CR}} \tag{9}$$

and the critical radius r_{CR} according to Eq. (8) lies in the range $0 < r_{CR} < \lambda_L/\alpha$ (Fig. 3). At the minimum of the curve

$$r_{CR} = \frac{1}{2}\frac{\lambda_L}{\alpha} \tag{10}$$

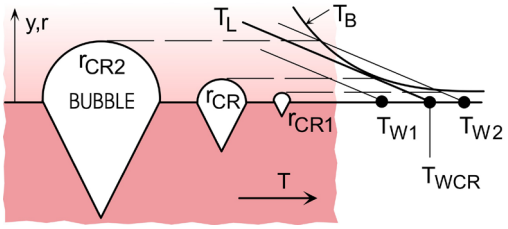

Fig. 2. Illustration of bubble growth criterion.

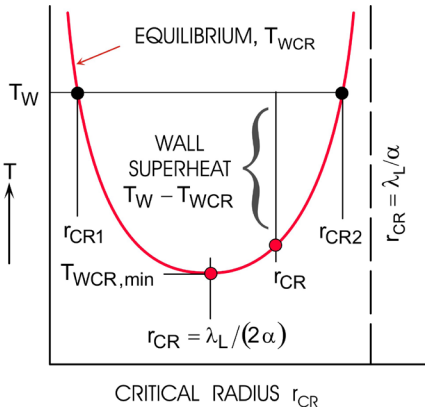

Fig. 3. Effect of wall temperature on critical bubble radius.

giving

$$T_{WCR,min} - T_\infty = 8\frac{\sigma T_\infty \alpha}{\Delta h \rho_V \lambda_L} = 4\frac{\sigma T_\infty}{\Delta h \rho_V r_{CR}} \tag{11}$$

For a specified wall temperature $T_W > T_{WCR}$, the spectrum of bubbles (size, radius) able to grow falls between r_{CR1} and r_{CR2} (Fig. 3). For any radius r_{CR} within this range, the temperature difference

$$T_W - T_{WCR} = T_W - T_\infty - 2\frac{\sigma T_\infty}{\Delta h \rho_V r_{CR}} \frac{1}{1 - \frac{\alpha r_{CR}}{\lambda_L}} \tag{12}$$

represents the wall superheat above the thermodynamic minimum. This temperature difference measures the shift of the system, including wall, liquid and the bubble, from its equilibrium state. Taking the temperature as a system coordinate, the temperature difference $T_W - T_{WCR}$ is a generalized force driving the system towards the equilibrium state.

This force is different for different bubble cavities. It is zero for $r_{CR} = r_{CR1}$ and $r_{CR} = r_{CR2}$, but maximum for r_{CR} given in Eq. (10)

$$T_W - T_{WCR,min} = T_W - T_\infty - 4\frac{\sigma T_\infty}{\Delta h \rho_V r_{CR}} \tag{13}$$

Any wall temperature above $T_{WCR,min}$, $T_W > T_{WCR,min}$, would suffice to generate vapour bubbles of a certain size. However, to suppress formation of viable bubbles, the wall temperature must not exceed the equilibrium temperature corresponding to the surface cavity of the mouth radius r_{CR}. Thus, the maximum temperature for pure convective falling film evaporation must be less than the minimum wall temperature required by the bubble equilibrium

$$T_{W,EVAP,max} \leq T_{W,NUCL,min} \tag{14}$$

or, involving Eq. (11)

$$T_{W,\mathrm{EVAP,max}} - T_{\infty} \le 8\frac{\sigma T_{\infty}\alpha}{\Delta h \rho_V \lambda_L} \tag{15}$$

To apply this equation to an evaporating liquid film, the temperature T_{∞} may be set equal to the interface temperature, which is practically the saturation temperature, $T_{\infty} = T_I = T_{\mathrm{EVAP}}$.

3. Effect of heat transfer on the wall temperature

According to Eq. (15), the maximum allowable wall temperature in falling film evaporators depends on the heat transfer in the film. Replacing in this equation the heat transfer coefficient $\alpha \equiv \alpha_{\mathrm{EVAP}}$ by the Nusselt number $\mathrm{Nu}_{\mathrm{EVAP}}$

$$\mathrm{Nu}_{\mathrm{EVAP}} = \frac{\alpha_{\mathrm{EVAP}}}{\lambda_L}\left(\frac{\nu_L^2}{g}\right)^{1/3} \tag{16}$$

gives

$$\frac{T_W - T_{\mathrm{EVAP}}}{T_{\mathrm{EVAP}}} \le 8\frac{\sigma}{\Delta h \rho_V}\left(\frac{g}{\nu_L^2}\right)^{1/3}\mathrm{Nu}_{\mathrm{EVAP}} \tag{17}$$

where the index EVAP,max in T_W has been omitted.

The temperature T_W is not easy accessible in the practice and shall be removed from the equations by involving Eqs.(1) and (2). With these, the temperature difference $T_W - T_{\mathrm{EVAP}}$ can be expressed as

$$T_W - T_{\mathrm{EVAP}} = \frac{T_{\mathrm{COND}} - T_{\mathrm{EVAP}}}{1 + \frac{\alpha_{\mathrm{EVAP}}}{\alpha_{\mathrm{COND}}} + \frac{\alpha_{\mathrm{EVAP}}\delta_W}{\lambda_W}}, \tag{18}$$

giving

$$\frac{T_{\mathrm{COND}} - T_{\mathrm{EVAP}}}{T_{\mathrm{EVAP}}} \le 8\cdot\left(1 + \frac{\alpha_{\mathrm{EVAP}}}{\alpha_{\mathrm{COND}}} + \frac{\alpha_{\mathrm{EVAP}}\delta_W}{\lambda_W}\right) \cdot\frac{\sigma}{\Delta h \rho_V}\left(\frac{g}{\nu_L^2}\right)^{1/3}\mathrm{Nu}_{\mathrm{EVAP}} \tag{19}$$

By this expression the temperature difference increases with increasing α_{EVAP} and decreasing α_{COND}. A reliable process operation requires the expression (19) to be fulfilled also at the minimum of the right-hand side, that is, for $\alpha_{\mathrm{COND}} \to \infty$ and/or $\alpha_{\mathrm{EVAP}} = 0$.

The condensation heat transfer depends on the thickness of the condensate film forming inside the evaporator tubes. Defining α_{COND} by

$$\alpha_{\mathrm{COND}} = \frac{\lambda_L}{\delta_{\mathrm{COND}}} \tag{20}$$

where λ_L is the thermal conductivity and δ_{COND} the thickness of the condensate film, the calculation of α_{COND} reduces to the calculation of δ_{COND}.

In general, the thickness of the condensate film is governed by the simultaneous actions of vapour shear and gravity, Mitrovic [22]. Near the vapour inlet, the vapour shear dictates the condensate flow, while towards the tube end, the effect of gravity predominates (Fig. 4). Neglecting the gravity effect in the vapour inlet region, the simplified momentum and energy balances for the condensate film deliver

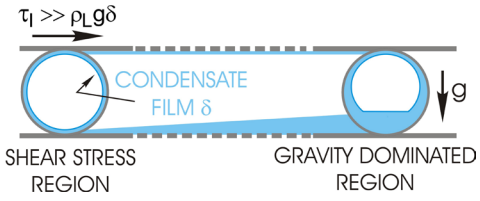

Fig. 4. Illustration of vapour condensation in a horizontal tube.

$$\delta_{\mathrm{COND}} = \left(3\frac{\lambda_L\left(T_{\mathrm{COND}} - T_W\right)\mu_L}{\tau_V \rho_L \Delta h} z\right)^{1/3} \tag{21}$$

$$\alpha_{\mathrm{COND}} = \left(\frac{1}{3}\frac{\lambda_L^2 \tau_V \rho_L \Delta h}{\left(T_{\mathrm{COND}} - T_W\right)\mu_L z}\right)^{1/3}. \tag{22}$$

At $z \to 0$, $\delta_{\mathrm{COND}} \to 0$, and $\alpha_{\mathrm{COND}} \to \infty$. The most favourable conditions for bubble formation in the falling film on the tube outside surface are thus expected in the region of vapour inlet, where Eq.(19) may be simplified to

$$\frac{T_{\mathrm{COND}} - T_{\mathrm{EVAP}}}{T_{\mathrm{EVAP}}} \le 8\cdot\left(1 + \frac{\alpha_{\mathrm{EVAP}}\delta_W}{\lambda_W}\right)\cdot\frac{\sigma}{\Delta h \rho_V}\left(\frac{g}{\nu_L^2}\right)^{1/3}\mathrm{Nu}_{\mathrm{EVAP}} \tag{23}$$

Replacing α_{EVAP} in Eq.(23) according to Eq.(16) gives

$$\frac{T_{\mathrm{COND}} - T_{\mathrm{EVAP}}}{T_{\mathrm{EVAP}}} \le 8\cdot\left(1 + \frac{\lambda_L}{\lambda_W}\left(\frac{\delta_W^3 g}{\nu_L^2}\right)^{1/3}\mathrm{Nu}_{\mathrm{EVAP}}\right) \cdot\frac{\sigma}{\Delta h \rho_V}\left(\frac{g}{\nu_L^2}\right)^{1/3}\mathrm{Nu}_{\mathrm{EVAP}} \tag{24}$$

For a sufficiently low thermal resistance of the tube wall, $\alpha_{\mathrm{EVAP}} << \lambda_W/\delta_W$, Eq.(23) becomes

$$\frac{T_{\mathrm{COND}} - T_{\mathrm{EVAP}}}{T_{\mathrm{EVAP}}} \le 8\cdot\frac{\sigma}{\Delta h \rho_V}\left(\frac{g}{\nu_L^2}\right)^{1/3}\mathrm{Nu}_{\mathrm{EVAP}}. \tag{25}$$

Eqs. (24) and (25) link the bubble formation conditions with the heat transfer in the falling film, the later being represented by $\mathrm{Nu}_{\mathrm{EVAP}}$.

If the condensation heat transfer resistance is to be taken into account, Eq.(19) must be used instead of Eq.(24), that is,

$$\frac{T_{COND}-T_{EVAP}}{T_{EVAP}} \le 8 \cdot \left(1+\left(\frac{\lambda_L}{\alpha_{COND}}\left(\frac{g}{\nu_L^2}\right)^{1/3}+\frac{\lambda_L}{\lambda_W}\left(\frac{\delta_W^3 g}{\nu_L^2}\right)^{1/3}\right)\mathrm{Nu}_{EVAP}\right) \cdot \frac{\sigma}{\Delta h \rho_V}\left(\frac{g}{\nu_L^2}\right)^{1/3}\mathrm{Nu}_{EVAP} \quad (26)$$

where α_{COND} represents the local value. This expression provides a possibility to specify the maximum allowable thermal potential driving the evaporation process. The two temperatures, T_{COND} and T_{EVAP}, are immediately accessible experimentally. Because of the dependency of the physical properties on the temperature, the expression is generally not explicit in $T_{COND} - T_{EVAP}$.

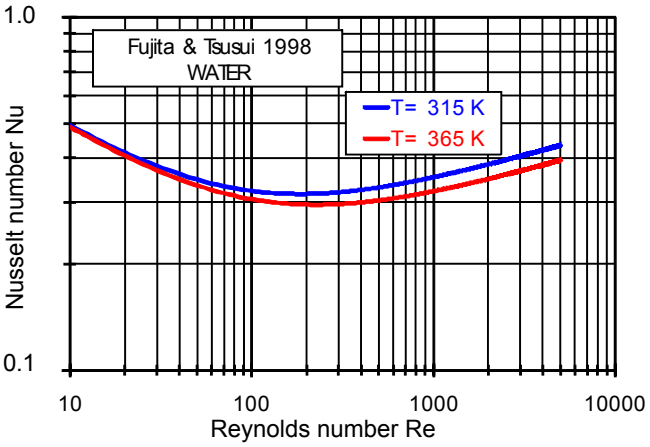

Fig. 5. Falling film Nusselt number according to Fujita and Tsusui [25], Eq.(27).

4. Illustration and discussion of results

In Eqs.(24) and (25), the Nu_{EVAP} represents the local Nusselt number of falling film. Depending on film flow pattern (Mitrovic [23]), this quantity varies not only on the tube circumference but also along the tube. Literature records do not provide a correlation for calculating the local Nusselt number for horizontal sprayed tubes. However, there are several correlations in the literature for the average heat transfer. Reviews have been performed e.g. by Mitrovic [24] and more recently by Ribatski and Jacobi [25]. For the present considerations, a correlation recommended by Fujita and Tsutsui [26] for each single tube of a vertical column of horizontal tubes is adopted:

$$\mathrm{Nu}_{EVAP}=\frac{\alpha_{EVAP}}{\lambda_L}\left(\frac{\nu_L^2}{g}\right)^{1/3}=\left(\mathrm{Re}^{-2/3}+0.01\cdot\mathrm{Re}^{0.3}\,\mathrm{Pr}_L^{0.25}\right)^{1/2} \quad (27)$$

where Pr_L is the Prandtl number and Re the Reynolds number of the film

$$\mathrm{Re}=4\frac{\dot{\Gamma}_{1/2}}{\mu_L} \quad (28)$$

$\dot{\Gamma}_{1/2}$ being the film flow rate on one tube side per unit of tube length.

Eq. (27) is applicable in the whole range of the Reynolds number (Fig. 5). The curves in Fig. 6 represent the driving thermal potential, $(T_{COND} - T_{EVAP}) / T_{EVAP}$, according to Eq. (25).

If scaled by the physical property group,

$$M=\frac{\sigma}{\Delta h \rho_V}\left(\frac{g}{\nu_L^2}\right)^{1/3} \quad (29)$$

Eq. (25) may be written as

$$\frac{1}{8}\frac{1}{M}\frac{T_{COND}-T_{EVAP}}{T_{EVAP}} \le \mathrm{Nu}_{EVAP} \quad (30)$$

This expression identifies the Nu_{EVAP}-curves in Fig. 5 as the upper boundary of the scaled thermal potential in a falling film evaporator equipped with thin-walled tubes, $\delta_W \to 0$, or with tubes having an extremely large thermal conductivity, $\lambda_W \to \infty$. As follows from Fig. 5, the curves pass minima at

$$\mathrm{Re}=278\cdot\mathrm{Pr}_L^{-0.26} \quad (31)$$

As the minimum of the driving temperature difference coincides with the minimum of the Nusselt number, the ranges of the Reynolds number near the values given by Eq. (31) should be avoided in the practice.

In light of the present considerations, the region of smaller Reynolds number may be recommended for the practice, if this recommendation does not conflict with other criteria of film rupture. Indeed, wetting criteria basing on theoretical models or experimental observations require the Reynolds number to lie above a threshold value. For instance, Lorenz and Yung [27] recommended on the basis of experiments with ammonia on a larger tube bundle (3000 tubes, arranged in 100 columns by 30 rows) the minimum Reynolds number of Re ≥ 300. This value almost coincides with the Reynolds number at the minimum of the Nussselt number (Fig. 5), and the requirement must be satisfied for any tube row, including the bottom bundle row.

Figs. 6–9 show the driving temperature differences as function of the Reynolds number according to Eq. (25) for two evaporation temperatures, namely 315 K and 365 K. The thickness of the tube wall is varied as parameter (δ_W = 1 mm, 0.5 mm, and 0 mm), which accounts for the effect of thermal resistance of the wall on the overall driving temperature difference, $T_{COND} - T_{EVAP}$. In general, the curves follow the shape $\mathrm{Nu}_{EVAP} = f$ (Re), showing minima in the laminar-turbulent transition region of the film flow. A larger wall thickness allows a larger

overall temperature difference, the boundary at $\delta_W = 0$ being of academic interest. The effect of the evaporation temperature on the allowable temperature difference is interesting regarding the level of the temperature difference. For instance, at the evaporation temperature of 315 K, the driving temperature difference lies above 10 K (between 10 K and 20 K), whereas at 365 K it lies between 2 K and 5 K. The increase of the allowable temperature difference at the decreased evaporation temperature is associated with the physical properties and processes that govern the bubble nucleation. As is well known both experimentally and theoretically, a lower evaporation temperature requires a higher wall superheat (wall temperature) for bubble inception. Being the part of the overall driving temperature difference, the required larger wall superheat (bubble nucleation temperature) at the lower evaporation temperature leads immediately to a larger allowable temperature difference $T_{COND} - T_{EVAP}$.

The results illustrated in Figs. 6–9 rest on the assumption of a negligible heat transfer resistance on the condensation side. This state is expected in the inlet region of heating vapour. Downstream this region, the heat transfer coefficient α_{COND} is finite which allows a larger driving temperature difference.

Eq. (26) is used to illustrate the effect of the inside (condensation) thermal resistance on the driving temperature difference. Figs. 10 and 11 show the effect of α_{COND} at the selected evaporation temperatures. The values of α_{COND} are selected to be: 5×10^3 W/(m^{2}K), 10×10^3 W/(m^{2}K) and 15×10^3 W/(m^{2}K). As expected, a smaller heat transfer coefficient corresponds to a larger temperature difference.

5. Conclusion

The results reported in the present paper illuminate a restriction regarding the evaporation rate in falling film apparatus associated with bubble nucleation. The equation derived for the minimum wall temperature required by bubble formation in the evaporating falling film formulates an operational heat transfer criterion.

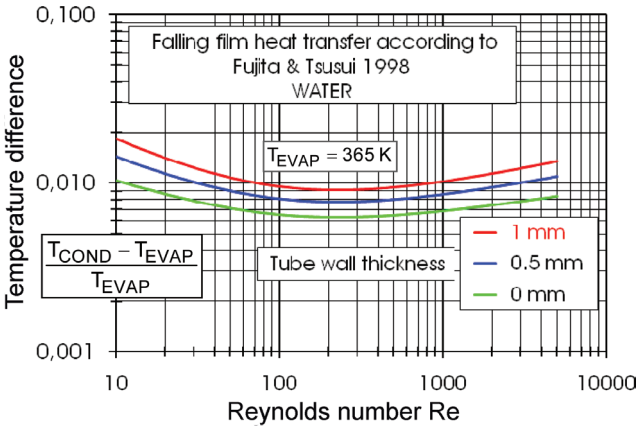

Fig. 6. Dimensionless maximum driving temperature difference, Eq.(25).

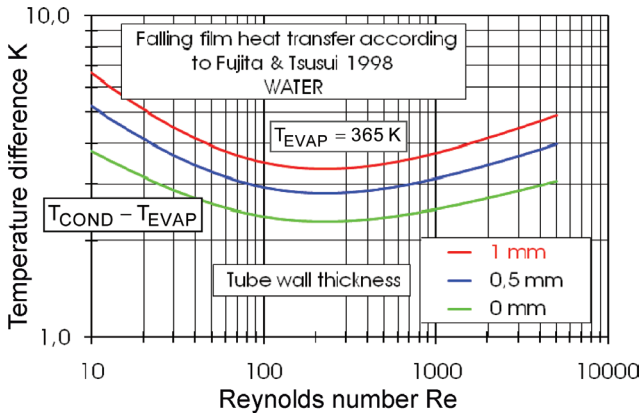

Fig. 7. Maximum driving temperature difference, Eq.(25).

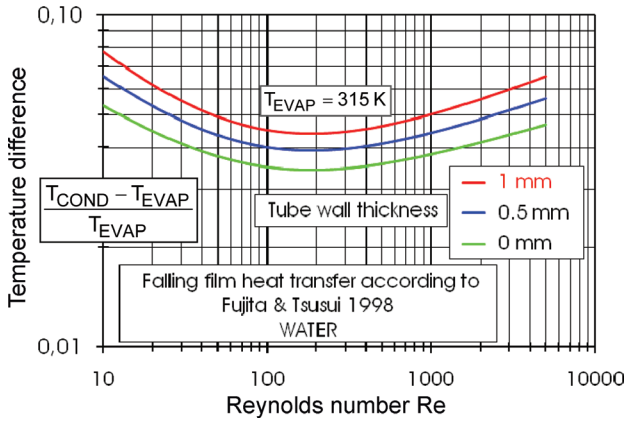

Fig. 8. Dimensionless maximum driving temperature difference, Eq.(25).

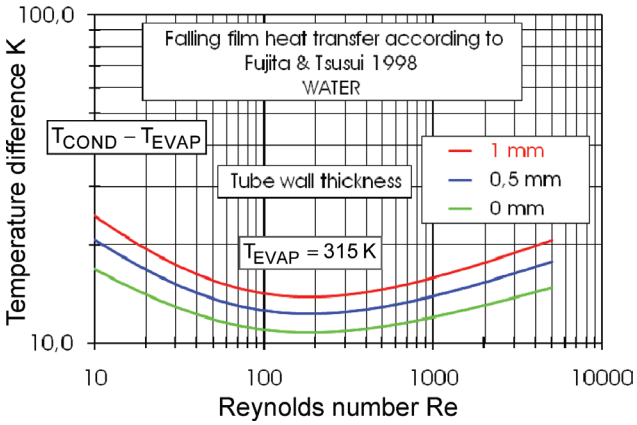

Fig. 9. Maximum driving temperature difference, Eq.(25).

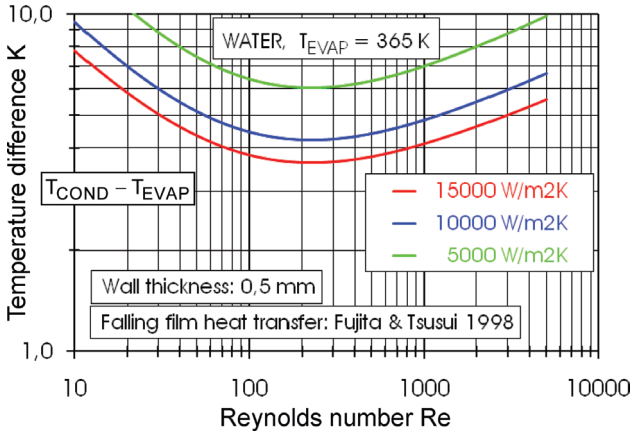

Fig. 10. Effect of condensation heat transfer on maximum driving temperature difference, Eq.(26).

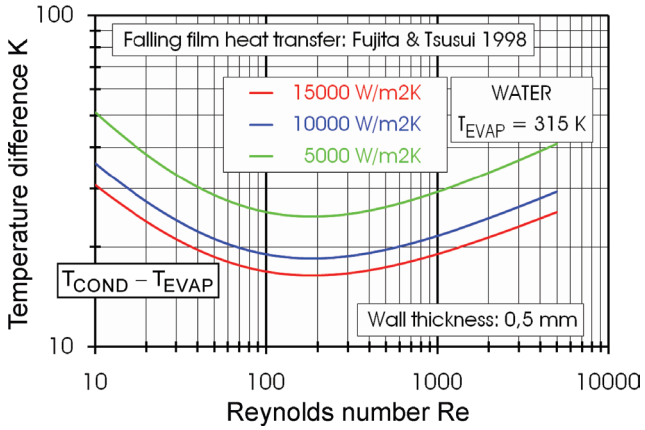

Fig. 11. Effect of condensation heat transfer on maximum driving temperature difference, Eq.(26).

As nucleation of vapour bubbles may lead to formation of dry patches, the minimum nucleation temperature defines the maximum allowable driving temperature difference for convective evaporation.

By this criterion, a larger driving temperature difference is allowable at a lower evaporation temperature. At a higher evaporation temperature, the falling film heat transfer increases bringing stronger the effect of the thermal resistance of the tube wall into the play. In multi-effect falling film desalination plants, the criterion equation derived in this paper allows separate formulations of process conditions in the respective effects for each tube.

Symbols

A — Interface area, m²
g — Acceleration due to gravity, m/s²
Δh — Enthalpy of phase change, J/kg
k — Overall heat transfer coefficient, W/(m²K)
M — Physical property group
$\dot{m}$ — Mass flux, kg/m²
Nu — Nusselt number
Pr — Pradntl number
q — Heat flux, W/m²
r — Radius, m²
Re — Reynolds number
T — Temperature, K
ΔT — Temperature difference, K
t — Time, s
u — Velocity, m/s
z — Coordinate along evaporator tube, m

Greek

α — Heat transfer coefficient, W/(m²K)
$\dot{\Gamma}_{1/2}$ — Liquid flow rate on one tube side per unit length, kg/(sm)
δ — Wall thickness, distance to wall, m
λ — Thermal conductivity, W/Km
ρ — Density, kg/m³
μ — Dynamic viscosity, Ns/m²
ν — Kinematic viscosity, m²/s
σ — Surface tension,N/m
τ — Shear stress, N/m²

Subscripts

B — Bubble
C — Cavity
CR — Critical
COND — Condensation
EVAP — Evaporation
L — Liquid
I — Interface
V — Vapour
W — Wall
∞ — Far from wall

References

[1] J.W. Westwater, Boiling of liquids, Adv. Chem. Eng., 1 (1956) 1-76.
[2] E.I. Nesis, Boiling of liquids, Soviet Physics Uspekhi, 8 (1966) 883-907.
[3] P. Van Carey, Liquid-Vapor Phase-Change Phenomena, Taylor and Francis, NY 1992.
[4] J.G. Collier and J.R. Thome, Convective Boiling and Condensation, Clarendon Press, Oxford, 1994.
[5] Y.-Y. Hsu and R.W. Graham, Transport Processes in Boiling and Two-Phase Systems, Hemisphere Pub. Corp., 1976.
[6] J. Mitrovic, How to create an efficient surface for nucleate boiling? Int. J. Thermal Sci., 45 (2006) 1–15.
[7] W. Thomson (Lord Kelvin), On the equilibrium of vapour at a curved surface of liquid, London, Edinburgh, Dublin Philos. Mag. J. Sci., Series 4, 42 (1871) 448–453.
[8] J.W. Gibbs, On the equilibrium of heterogeneous substances, Trans. Connecticut Acad. Arts Sci., 3 (1874–1878) 108–248.
[9] J.J. Thomson, Applications of Dynamics to Physics and Chemistry, London, 1886.

[10] J. Mitrovic, On the equilibrium conditions of curved interfaces, Int. J. Heat Mass Transfer, 47 (2004) 809-818.
[11] J.D. Van der Waals, The thermodynamic theory of capillarity under the hypothesis of a continuous variation of density, (Translation by J.S. Rowlinson), J. Stat. Phys., 20 (1979) 197–224.
[12] R.J. Boscovich, Theoria Philosophiae Naturalis, Venetiis, 1763, English translation by J.M. Child, A Theory of Natural Philosophy, M.I.T. Press, 1921.
[13] J. Mitrovic, On the profile of the liquid wedge underneath a growing vapour bubble and the reversal of the wall heat flux, Int. J. Heat Mass Transfer, 45 (2002) 409-415.
[14] M. Jakob and W. Fritz, Versuche über den Verdampfungsvorgang, Fors. Gebiet des Ingenieur., 2 (1931) 435-447.
[15] C. Corty and A.S. Foust, Surface variables in nucleate boiling, Chem. Eng. Progress Sym. Ser., 51(17) (1955) 1–12.
[16] J. Aitken, On boiling, condensing, freezing, and melting, Trans. Royal Scottish Soc. Arts, Edinburgh, 9 (1878) 240-287.
[17] Y.Y. Hsu, On the size range of active nucleation cavities on a heating surface, ASME J. Heat Transfer, 84C (1962) 207–216.
[18] J. Mitrovic, Phase equilibrium of a liquid droplet formed on a solid particle, Chem. Eng. Sci., 61 (2006) 5925–5933.
[19] P. Griffith and J.D. Wallis, The role of surface conditions in nucleate boiling, Chem. Eng. Progress, Sym. Ser.,56(30) (1960) 49–63.
[20] W.M. Rohsenow, Status of and problems in boiling and condensation heat transfer, Progress Heat Mass Transfer, 6 (1972) 1–44.
[21] J.R. Howell and R. Siegel, Activation, Growth, and Detachment of Boiling Bubbles in Water from Artificial Nucleation Sites of Know Geometry and Size, NASA TN-D 4101, 1967.
[22] J. Mitrovic, Condensation Heat Transfer (in preparation), 2010.
[23] J. Mitrovic, Flow structures of a liquid film falling on horizontal tubes, Chem. Eng. Technol., 28 (2005) 684–694.
[24] J. Mitrovic, Heat transfer on sprayed horizontal tubes, VDI Düsseldorf, Ser. 3, No. 211, 1990.
[25] G. Ribatski and A.M. Jacobi, Falling-film evaporation on horizontal tubes — a critical review, Int. J. Refrigeration, 28 (2005) 635–653.
[26] Y. Fujita and M. Tsutsui, Experimental Investigation of falling film evaporation on horizontal tubes, Heat Transfer – Japan. Res., 27 (1998) 609–618.
[27] J.J. Lorenz and D. Yung, Film breakdown and bundle-depth effects in horizontal-tube, falling-film evaporators, ASME J. Heat Transfer, 104 (1982) 569–571.